Hybrid mesoporous nanocarriers act by processing logic tasks: Toward the design of nanobots capable of reading information from the environment

Antoni Llopis-Lorente,[a,b,c] *Beatriz de Luis,*[a,b,c] *Alba García-Fernández,*[a,c,d] *Sandra Jiménez-Falcao,*[e] *Mar Orzáez,*[d] *Félix Sancenón,*[a,b,c] *Reynaldo Villalonga*[*e] *and Ramón Martínez-Máñez*[*a,b,c]

[a] Instituto de Reconocimiento Molecular y Desarrollo Tecnológico (IDM), Unidad Mixta Universidad Politécnica de Valencia-Universidad de Valencia (Spain).

[b] Departamento de Química, Universidad Politécnica de Valencia. Camino de Vera s/n, 46022, Valencia (Spain).

[c] CIBER de Bioingeniería, Biomateriales y Nanomedicina (CIBER-BBN) (Spain).

[d] Centro de Investigación Príncipe Felipe. Eduardo Primo Yúfera 3, 46012, Valencia (Spain).

[e] Nanosensors & Nanomachines Group, Department of Analytical Chemistry, Faculty of Chemistry, Complutense University of Madrid, 28040, Madrid (Spain).

KEYWORDS

biocomputing • nanorobots • logic gates • mesoporous nanoparticles • drug delivery

ABSTRACT

Here we present the design of smart nanodevices capable of reading molecular information from the environment and acting accordingly by processing boolean logic tasks. As proof of concept, we prepared Au-mesoporous silica (MS) nanoparticles functionalized with the enzyme glucose dehydrogenase (GDH) on the Au surface and with supramolecular nanovalves as caps on the MS surface, which is loaded with a cargo (dye or drug). The nanodevice acts as an AND logic gate and reads information from the solution (presence of glucose and nicotinamide adenine dinucleotide (NAD^+)), which results in cargo release. We show the possibility of co-immobilizing GDH and the enzyme urease on nanoparticles to mimic an INHIBIT logic gate, in which the AND gate is switched off by the presence of urea. We also show that such nanodevices can deliver cytotoxic drugs in cancer cells by recognizing intracellular NAD^+ and the presence of glucose.

INTRODUCTION

A novel and ambitious approach in the nanotechnology field is to design smart nanobots (or nanorobots). Research activities in nanobotics comprise an emerging interdisciplinary technology area with new scientific challenges and promising revolutionary advancement in medicine.[1] Nanobots can be made by assembling abiotic and/or biological nanocomponents, and can be considered as a possible way to enable the required manufacturing technology to move toward a new generation of smart nanodevices for applications such as drug delivery or diagnosis.[2] An appealing feature of such futuristic systems is their potential ability to read information from the environment (e.g., diseased tissues or interior of cells) and to act accordingly. Inputs can, for instance, be combinations of certain molecules which abnormal

levels can be indicative of a health disorder. As for macroscale devices, logic operators[3] could be potentially used to control nanobots capable of processing (bio)chemical inputs and producing outputs, like drug delivery, inducing apoptosis, etc. Logic gates are operators used in electronics to process two binary inputs or more, and produce a single binary output.[4] Current digital computers and electronic devices are programmed to process information inputs using algorithms based on logic gates. Although electronic logic gates cannot be incorporated into nanoparticles, one possible approach could be to use chemical systems that mimic the operation of their electronic counterparts.[5-8] Transferring these computing capabilities to nanoscale machines in relation to reading information from the environment is a key step to build advanced biomedical nanobots capable of performing complex tasks in biological settings.

From another point of view, stimuli-responsive delivery systems have recently gained much interest due to their potential application to develop better medical therapies and sensing protocols. Researchers are exploring the use of liposomes, metallic nanoparticles and polymeric and inorganic materials as potential drug carriers.[9-12] Among them, mesoporous silica (MS) materials are appealing given their high loading capacity, stability, biocompatibility, and the possibility to functionalize them with molecular gates or nanovalves on their outer surface.[13-17] These molecular gates are molecular or supramolecular ensembles that prevent the cargo from being released until an external stimulus is applied. Gated mesoporous materials responsive to physical (such as light, temperature, magnetic fields)[18-20] and chemical (such as pH, enzymes, redox agents and chemical species)[21-27] stimuli have been reported. However, comparatively few materials respond to small molecules of biological interest and, when this is the case, it is usually the presence of a single molecule to which the system responds.[16] In contrast, delivery nanodevices capable of reading information from the environment and delivering the cargo in

Boolean logic terms with more than a single input are rare. However, the conceptual design (Figure 1) of such systems is interesting since diseases usually produce abnormal levels of a combination of molecules.[28-29]

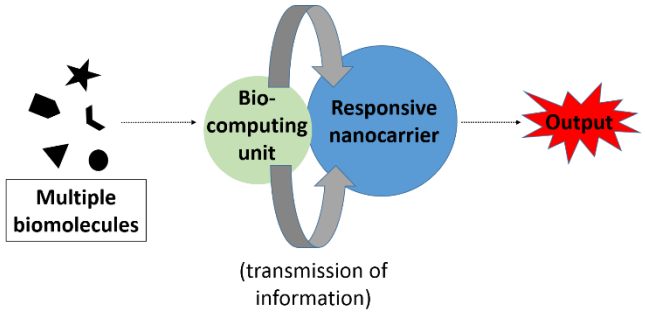

Figure 1. Conceptual representation of a smart nanodevice equipped with a biocomputing unit (capable of reading and processing molecular information from the environment and sending a chemical messenger to a responsive nanocarrier unit which can deliver a cargo (dye or drug)).

Given the potential benefits of developing nanodevices capable of sensing molecular information from the environment, we report herein the preparation of nanoparticles equipped with enzymatic logic gates that are able to perform biocomputing operations which result in the programmed delivery of an entrapped cargo. The systems consist of Janus nanoparticles with gold and MS on opposites surfaces. The MS surface is loaded with a cargo (a dye or a drug) and is functionalized with a pH-responsive β-cyclodextrin (β-CD):benzimidazole supramolecular nanovalve. The Au surface acts as a biocomputing unit and contains enzymes capable of "detecting" the simultaneous presence of certain biomolecules and transforming information into a local chemical messenger that is able to open the β-CD:benzimidazole nanovalve and induce cargo delivery. Based on this concept, nanoparticles that display AND or INHIBIT logic behavior are prepared (Figure 2). In particular, the AND system contains the enzyme glucose

dehydrogenase (GDH) and responds to the simultaneous presence of glucose and nicotinamide adenine dinucleotide (NAD^+). Although several glucose-responsive delivery systems have been reported,[30-32] they usually respond to the single presence of glucose which is found in both extra- and intra-cellular environments. NAD^+ is found in the interior of living cells where it participates as a cofactor in a number of enzymatic reactions. Furthermore, both glucose uptake and NAD^+/NADH ratio are increased in cancer cells.[33,34] Thus, nanocarriers capable of performing AND logic analysis of glucose and NAD^+ could be advantageous for the construction of more selective (glucose-responsive) delivery systems. Additionally, we also report the possibility of co-immobilizing GDH and the enzyme urease on nanoparticles to mimic an INHIBIT logic gate, in which the AND gate is switched off by the presence of urea. Urea is a key biomolecule which is synthesized in liver cells and transported in the blood to the kidneys. Programming nanocarriers with INHIBIT-logic functions could potentially be useful to design smart delivery systems that are switch off in particular regions or cells where certain biomolecules are expressed.

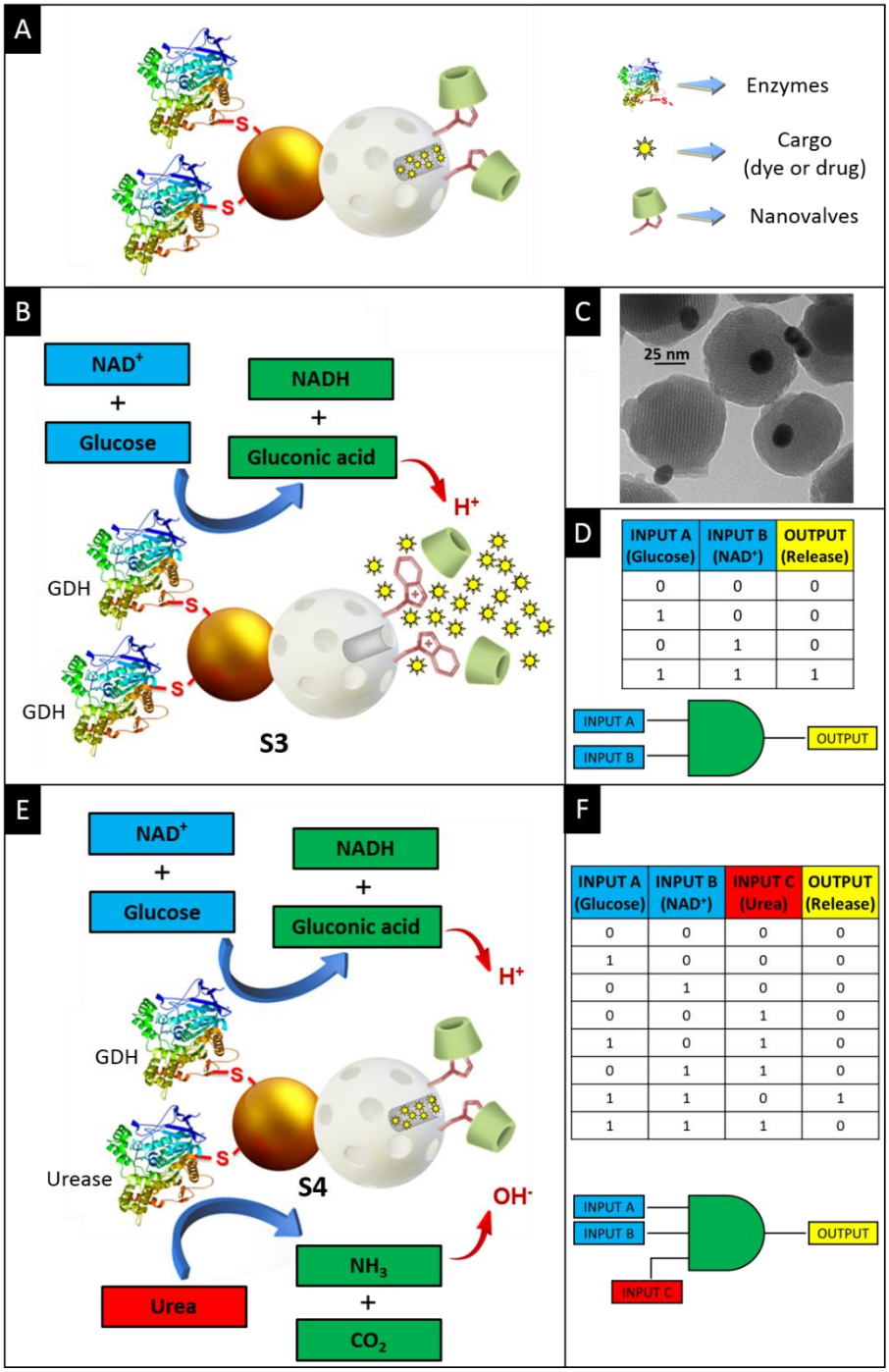

Figure 2. The nanoparticles reported in this paper. (A) General representation. (B) Nanoparticles **S3** with an AND logic behavior**.** The combination of both inputs (glucose and NAD^+) is recognized by the biocomputing unit resulting in cargo release from the mesoporous surface. (C) The TEM image of the Au-MS scaffold **(S1)**. (D) The Boolean logic table and scheme for an AND logic gate, as used in computing and electronics. (E) Representation of nanoparticles **S4** with an INHIBIT logic behavior. The system is switched off by the presence of urea. (F) The Boolean logic table and scheme for an INHIBIT logic gate, as used in computing and electronics.

RESULTS AND DISCUSSION

Mesoporous silica nanoparticles (**MSNPs**) were synthesized by a standard procedure, which employs cetyltrimethylammonium bromide (CTAB) as a directing agent for the condensation of inorganic precursor tetraethyl orthosilicate (TEOS) in basic media. The as-synthesized **MSNPs** were calcined in air to remove the surfactant. Gold nanoparticles (**AuNPs**) were synthesized by reducing Au(III) with sodium citrate. In another step, **MSNPs** were confined at the interface of a paraffin-water emulsion to partially functionalize them with (3-mercaptopropyl)trimethoxysilane (see Supporting Information for details). **AuNPs** and **MSNPs** were then attached by the formation of S-Au bonds, which yielded the Janus Au-MS nanoparticles (**S1**). **S1** was loaded with the fluorophore $[Ru(bpy)_3]Cl_2$ and the outer silica surface was functionalized with benzimidazole moieties by the nucleophilic substitution of the previously anchored (3-iodopropyl)trimethoxysilane. The gold surface was functionalized with carboxylic groups by a treatment with 3-mercaptopropionic acid, which finally yielded **S2**. The resulting nanoparticles were capped with β-CD, which forms inclusion complexes ($K_f = 104\ M^{-1}$)[35] with benzimidazole (**S2-CD**). Finally, enzyme glucose dehydrogenase (GDH) was linked to carboxylic groups on the gold surface by using N-hydroxysuccinimide and ethyl(dimethylaminopropyl) carbodiimide, which yielded the final nanodevice **S3**. Additionally, the co-immobilization of GDH and urease yielded the nanodevice **S4.**

The prepared materials were characterized by standard procedures. The TEM images of Janus nanoparticles **S1** showed spherical **MSNPs** (ca. 100 nm) attached to **AuNPs** of ca. 20 nm (Figure 2-C and Figure S1). The as-synthesized **AuNPs** showed an absorption maximum at 523 nm, which was red-shift in Au-MSNPs (**S1**) to 533 nm due to the change in the refractive index around the gold nanospheres because of the MS attachment (Figure S3). The powder X-ray

diffraction (PXRD) patterns of the starting **MSNPs** and **S1** showed the characteristic (100) reflection peak of mesoporous silica around 2.4° (Figure S4). The preservation of this typical peak in **S2** confirmed that the cargo loading and surface functionalization processes did not damage the mesoporous scaffolding. Characteristic cubic gold peaks were observed at high-angle PXRD for **S1** and **S2**, which thus confirmed the presence of gold nanoparticles in these materials. From the N_2 adsorption-desorption isotherms (Figure S5), the total surface area of the starting **MSNPs** was 1018.70 $m^2 \cdot g^{-1}$, which diminished to 846.10 $m^2 \cdot g^{-1}$ for **S1** and to 123.24 $m^2 \cdot g^{-1}$ for **S2**. Pore size and pore volume were calculated by applying the BJH model to the adsorption band of the isotherm, and are summarized in Table S2. From the elemental analysis (Table S3 and S4), the contents of benzimidazole, cargo and β-CD in mmol per gram of **S2-CD** were determined as 0.28 (3.3 wt%), 0.08 (4.3 wt%) and 0.10 (11.2 wt%), respectively. The activity of immobilized enzyme on **S3** was determined as 1.25 $U \cdot mg^{-1}$, which corresponds to 17.91 mg of GDH per g of solid (Figure S6). TEM-EDX mapping of the final nanodevice **S3** was also carried out (Figure S2).

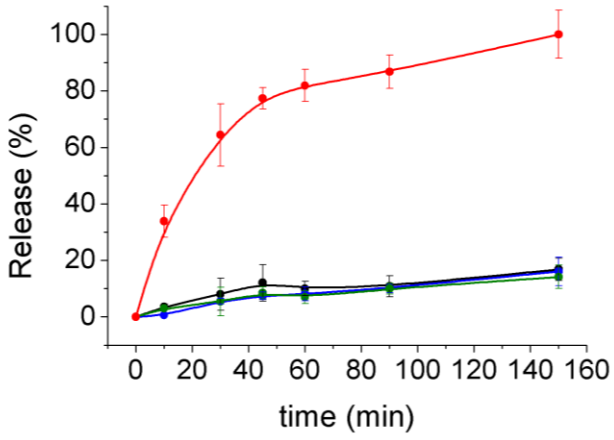

Figure 3. Normalized cargo release from **S3** determined by measuring $[Ru(bpy)_3]Cl_2$ fluorescence at 595 nm (λ_{exc} = 453 nm) *versus* time in aqueous solutions at pH 7.5: (black) in the absence of any input (0,0); (blue) in the presence of glucose (1,0); (green) in the presence of NAD^+ (0,1); (red) in the presence of both NAD^+ and glucose (1,1). Substrates added at 1 mM concentration. Error bars as σ from three independent experiments.

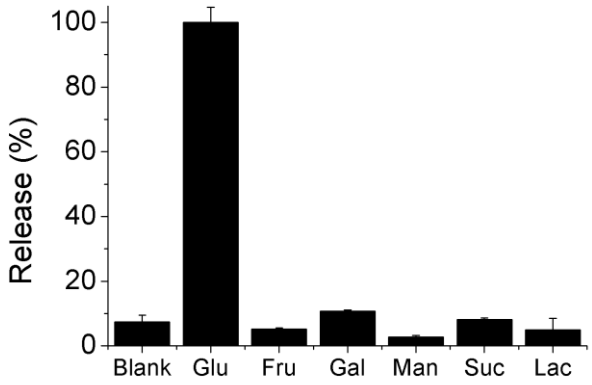

Figure 4. Normalized cargo release from **S3** in the presence of NAD^+ and different saccharides (glucose (Glu), fructose (Fru), galactose (Gal), mannose (Man), sucrose (Suc) and lactose (Lac)) at 1 mM concentration after 60 min. Error bars as σ from three independent experiments.

S3 was designed to monitor the environment and to deliver the cargo in the presence of glucose and NAD^+ following an AND logic behavior. In a typical experiment, **S3** was brought to 1 $mg{\cdot}mL^{-1}$ concentration in an aqueous solution at pH 7.5 upon the application of different conditions: absence of glucose and NAD^+ (0,0), presence of both (1,1), and presence of only glucose (1,0) or only NAD^+ (0,1). Aliquots were taken at the scheduled times, centrifuged to remove nanoparticles, and the cargo release was evaluated by measuring the emission band of $[Ru(bpy)_3]Cl_2$ at 595 nm (λ_{exc} = 453 nm). The obtained payload delivery kinetics are shown in Figure 3. In the absence of both inputs (0,0), and in the presence of only glucose (1,0) or only NAD^+ (0,1), **S3** was capped and the cargo release was lower than 10% after 2.5 h. However, when **S3** sensed the presence of glucose and NAD^+ (1,1) a subsequent remarkable cargo delivery took place. This was attributed to GDH recognizing both substrates (glucose and NAD^+). GDH catalyzed the reaction between glucose and NAD^+ to give glucono-1,5-lactone and NADH. Glucono-1,5-lactone hydrolyzed in water to give gluconic acid (pK_a = 3.6) (internal chemical messenger), which induced the protonation of the benzimidazole groups (pK_a = 5.55)[36] on the

MS surface, and the dethreading of the supramolecular nanovalve finally resulted in cargo delivery. NADH formation from glucose and NAD^+ in the presence of **S3** was confirmed (Figure S5). Moreover, it was also confirmed that the cargo delivery from **S3** in the presence of NAD^+ was observed only with glucose, but not with other saccharides, such as fructose, galactose, mannose, sucrose and lactose (Figure 4).

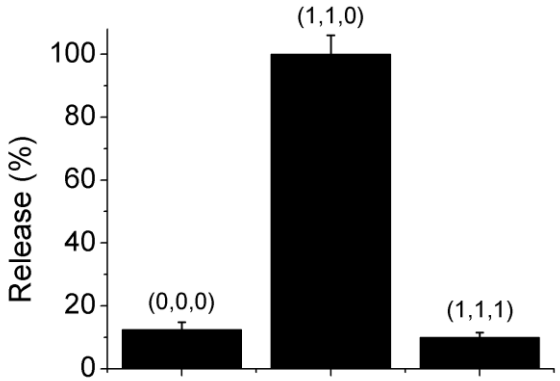

Figure 5. The INHIBIT-like behavior of **S4**. Normalized cargo release from **S4** in the absence of inputs (0,0,0); in the presence of glucose and NAD^+ and absence of urea (1,1,0); and in the presence of glucose, NAD^+ and urea (1,1,1) after 150 min. Substrates added at 1 mM concentration.

In another next step we aimed to prepare a nanodevice capable of reading from the environment three different molecules that control cargo delivery. In this scenario, we constructed nanodevice **S4,** in which GDH and the enzyme urease were co-immobilized on the gold surface (Figure 2E). The amount of GDH immobilized on **S4** lowered to 9.87 $mg \cdot g^{-1}$ (compared to 17.91 $mg \cdot g^{-1}$ for **S3**) as a result of urease co-immobilization (Figure S6). Nanodevice **S4** mimicked an INHIBIT logic gate in which the AND gate was switched off by urea. In Boolean logic terms, an INHIBIT gate is represented as shown in Figure 2-F; input C (urea) disables the gate (no output signal) even if input A (glucose) and B (NAD^+) are present. However, in a 0 state (absence) of the inhibit input C (urea), the gate is enabled and the output is

1 (cargo delivery is observed) when both input A (glucose) and input B (NAD^+) are in state 1 (present). INHIBIT gates are used when logic signals are needed to be either enabled or inhibited, depending on certain control inputs. In order to demonstrate the nanodevice's INHIBIT-like behavior, the release of **S4** suspensions (1 $mg \cdot ml^{-1}$) in the presence of (i) no inputs, (ii) glucose and NAD^+ and (iii) urea, glucose and NAD^+ after 150 min was evaluated. As seen in Figure 5, whereas a remarkable release occurred in the presence of glucose and NAD^+ (1,1,0), dye delivery became negligible when urea was also added (1,1,1). This was ascribed to the presence of urease on **S4,** which catalyzed the transformation of urea into CO_2 and two equivalents of NH_3. The produced ammonia induced an increase in pH in the microenvironment of the nanoparticles and neutralized the effect of gluconic acid, thus, inhibiting the release from the nanoparticles. With **S3**, addition of urea had no effect on the release (Figure S8), which indicated the key role played by urease in **S4**.

Encouraged by these findings, we aimed to demonstrate that such nanodevices can also read information, and act accordingly, in complex biological settings, such as cells. To this end, we prepared $\mathbf{S3_{DOX}}$ (similar to **S3,** but loaded with the cytotoxic drug doxorubicin) and tested its performance in human cervix adenocarcinoma (HeLa) cells. For these experiments, glucose was added as an external input, whereas the NAD^+ naturally produced in the cell interior was expected to be the second input. Controlled doxorubicin release from $\mathbf{S3_{DOX}}$ was studied by confocal microscopy by tracking doxorubicin-associated fluorescence, and also by cell viability assays. For confocal microscopy experiments, HeLa cancer cells were incubated with 50 $mg \cdot mL^{-1}$ of $\mathbf{S3_{DOX}}$ for 30 min, washed to remove non internalized nanoparticles and were further incubated with and without glucose (25 mM) for 24 h. Representative images of the doxorubicin release (red), DNA marker Hoechst 3342 (blue) and merge for HeLa cells under different

conditions are shown in Figure 6-I. In the presence of glucose (and intracellular NAD^+), a significant doxorubicin release was observed (Figure 6-Ib). In marked contrast, in the absence of glucose the doxorubicin release became negligible (Figure 6-Ic). Additionally, the WST-1 cell viability assays correlated well with the confocal microscopy studies. As seen in Figure 6-II, treating HeLa cells with $\mathbf{S3_{DOX}}$ in the presence of both glucose and intracellular NAD^+ led to cell viability considerably diminishing due to the doxorubicin release. When no glucose input was applied, no reduction in cell viability was observed. Therefore, these results confirmed that nanodevice $\mathbf{S3_{DOX}}$ is able to read conditions in competitive media (presence of glucose and NAD^+) and to deliver a cytotoxic drug to reduce cell viability. In addition, in order to confirm that the decrease in cell viability was due to doxorubicin release from $\mathbf{S3_{DOX}}$ and not to the acidic pH induced by the generated gluconic acid, we carried out additional viability experiments with $\mathbf{S3_{Blank}}$ (a solid similar to $\mathbf{S3_{DOX}}$ but without doxorubicin). Unlike $\mathbf{S3_{DOX}}$, $\mathbf{S3_{Blank}}$ did not produce any reduction in cell viability in the simultaneous presence of glucose and intracellular NAD^+ (Figure S9). On the other hand, although assessing the concentration of these elements in the body is difficult, it has been reported that glucose intracellular concentration is between 0-1 mM,[37,38] and that the ratio between free NAD^+ and NADH in the cytoplasm is about 700,[39,40] with an estimated NAD^+ concentration of 0.3 mM.[41,42] However, it is known that in cancer cells glucose uptake is considerably increased[33] and the redox ratios NAD^+/NADH and $NADP^+$/NADPH are about 5-10 times higher.[34] In this scenario, advanced nanobots functionalized with targeting agents and capable of performing glucose-NAD^+ logic sensing could be an interesting tool as therapeutic agents.

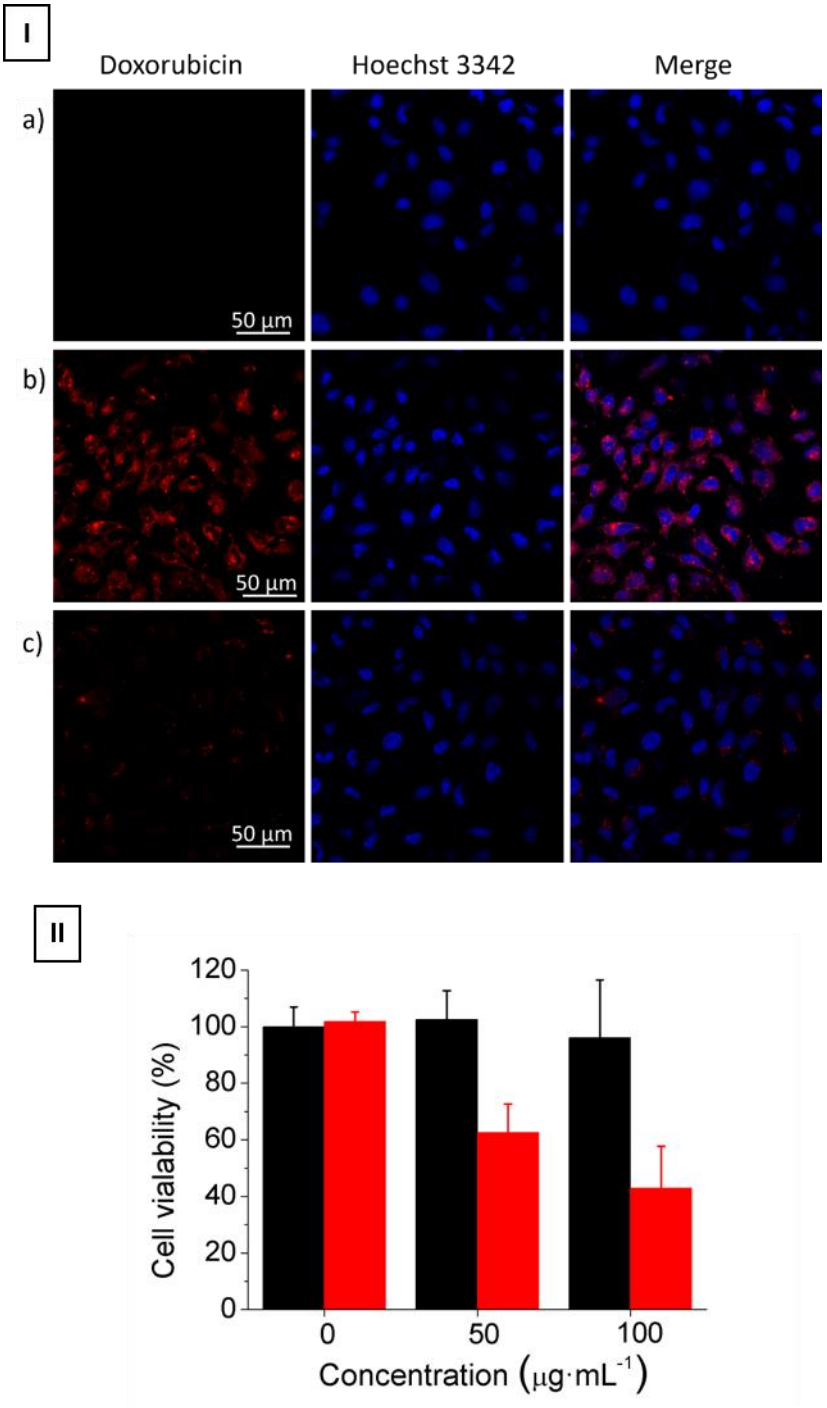

Figure 6. Experiments in cellular media. Top (I): confocal microscopy images of HeLa cells showing the controlled doxorubicin release from nanodevice **$S3_{DOX}$.** a) HeLa cells with no treatment; b) HeLa cells treated with 50 $\mu g \cdot mL^{-1}$ of **$S3_{DOX}$** in a medium containing glucose (25 mM); c) HeLa cells treated with 50 $\mu g \cdot mL^{-1}$ of **$S3_{DOX}$** in the absence of glucose. From left to right: doxorubicin fluorescence, DNA marker (Hoechst 3342) fluorescence and combined (merge). Bottom (II): cell viability assays of HeLa cells treated with different **$S3_{DOX}$** concentrations (0, 50 and 100 $\mu g \cdot mL^{-1}$) in the absence (black bars) or presence (red bars) of glucose (25 mM). Data shown as m±σ.

CONCLUSIONS

In conclusion, we show here the design of smart nanodevices capable of reading information from the environment (presence of glucose, NAD^+ and urea) and performing basic boolean logic tasks that result in the programmed delivery of an entrapped cargo. Nanoparticles with AND or INHIBIT logic behavior were prepared. The Au-MS nanoparticles functionalized with the enzyme GDH on the gold surface and with supramolecular pH-responsive nanovalves on the MS surface mimicked an AND logic gate and required two biomolecules (glucose and NAD^+) to trigger cargo release. Specificity was due to the incorporation of GDH, which transformed glucose and NAD^+ into gluconic acid and NADH. Gluconic acid acted as a local chemical messenger that induced the protonation of benzimidazole in the nanovalve, which disrupted the supramolecular complex and induced cargo delivery. We also found that two enzymes (GDH and urease) can be combined in a single nanodevice to display a more complex behavior. When urease and GDH were co-immobilized, the system acted as an INHIBIT logic gate, in which the AND gate was switched off and on by the presence or absence of urea. We also showed that the nanoparticles can deliver a cytotoxic drug in cancer cells after "detecting" the presence of glucose and intracellular NAD^+ in the environment. Given that multiple small biomolecules are altered in diseased cells and the number of enzymes that can be tested, we hope that our results inspire the development of smart programmed nanobots for medical applications such as drug delivery. We believe that the systems reported herein could allow advances to be made in our knowledge of how molecular information recognition (via simple chemical or biochemical reactions) can be converted into specific actions of nanodevices.[43,44] The idea of having nanodevices capable of sensing the environment and acting accordingly (processing logic tasks) embraces an enormous potential for the design of more advanced complex nanoscale systems

governed by the presence of multiple (bio)molecules and it could a promising first step to enable future nanoprocessors with increased complexity. Inspired by how biological communities sense the environment and act,[45] developing such nanodevices may open up new directions in nanobotics with a number of applications in different areas.

ASSOCIATED CONTENT

Supporting Information. Experimental procedures and further materials characterization.

AUTHOR INFORMATION

Corresponding Authors

*E-mail: rmaez@qim.upv.es

*E-mail: rvillalonga@quim.ucm.es

Author Contributions

The manuscript was written through contributions of all authors. All authors have given approval to the final version of the manuscript.

Notes

The authors declare no competing financial interest.

ACKNOWLEDGMENTS

A. Llopis-Lorente is grateful to "La Caixa" Banking Foundation for his PhD grant. A. García-Fernández thanks the Spanish government for her FPU fellowship. The authors are grateful to

the Spanish Government (MINECO Projects MAT2015-64139-C4-1, CTQ2014-58989-P and CTQ2015-71936-REDT) and the Generalitat Valencia (Project PROMETEOII/2014/047 and PROMETEOII/2014/061) for support. The Comunidad de Madrid (S2013/MIT-3029, Programme NANOAVANSENS) is also gratefully acknowledged.

REFERENCES

(1) Kwon, E. J.; Lo, J. H.; Bhatia, S. N. Smart Nanosystems: Bio-Inspired Technologies that Interact with the Host Environment. *PNAS* **2015**, *112*, 14460-14466.

(2) Hauert, S.; Bhatia, S. N. Mechanisms of Cooperation in Cancer Nanomedicine: Towards Systems Nanotechnology. *Trends Biotech.* **2014**, *32*, 448-455.

(3) Deschamps, J. P.; Valderrama, E.; Terés, L. *Digital Sytems: From Logic gates to Processors*, Springer, **2017,** pp. 21-41.

(4) Blundell, B. G.; Khan, N.; Lasebae, A.; Jabbar, M. *Computer Systems and Networks*, Thomson Learning: London, **2007**, pp. 17-39.

(5) Filo, O.; Lotan, N. *Information Processing by Biochemical Systems: Neural Network-Type Configurations*, Wiley: New Jersey, **2010**.

(6) Guliyev, R.; Ozturk, S.; Kostereli, Z.; Akkaya, E. U. From Virtual to Physical: Integration of Chemical Logic Gates. *Angew. Chem. Int. Ed.* **2011**, *50*, 9826-9831.

(7) Katz, E.; Privman, V. Enzyme-Based Logic Systems for Information Processing. *Chem. Soc. Rev.* **2010**, *39*, 1835-1857.

(8) Seelig, G.; Soleveichik, D.; Zhang, D. Y.; Winfree, E. Enzyme-Free Nucleic Acid Logic Circuits. *Science* **2006**, *314*, 1585-1590.

(9) Kamaly, N.; Yameen, B.; Wu, J.; Farokhzad, O. C. Degradable Controlled-Release Polymers and Polymeric Nanoparticles: Mechanisms of Controlling Drug Release. *Chem. Rev.* **2016**, 116, 2602.

(10) Mura, S.; Nicolas, J.; Couvreur, P. Stimuli-Responsive Nanocarriers for Drug Delivery. *Nat. Mater.* **2013**, *12*, 991-1003.

(11) Mathiyazhakan, M.; Wiraja, C.; Xu, C. A Concise Review of Gold Nanoparticles-Based Photo-Responsive Liposomes for Controlled Drug Delivery. *Nano-Micro Lett.* **2018**, *10*, 1-10.

(12) Knezevic, N. N. Z.; Durand, J.-O. Large Pore Mesoporous Silica Nanomaterials for Application in Delivery of Biomolecules. *Nanoscale* **2015**, *7*, 2199-2209.

(13) Croissant, J. G.; Fatieiev, Y.; Almalik, A.; Khashab, N. Mesoporous Silica and Organosilica Nanoparticles: Physical Chemistry, Biosafety, Delivery Strategies, and Biomedical Applications. *Adv. Healthcare Mater.* **2017**, *7*, 1700831.

(14) Castillo, R. R.; Colilla, M.; Vallet-Regí, M. Advances in Mesoporous Silica-Based Nanocarriers for Co-Delivery and Combination Therapy against Cancer. *Expert. Opin. Drug Deliv.* **2017**, *14*, 229-243.

(15) Tarn, D.; Ashley, C. E.; Xue, M.; Carnes, E. C.; Zink, J. I.; Brinker, C. J. Mesoporous Silica Nanoparticle Nanocarriers: Biofunctionality and Biocompatibility. *Acc. Chem. Res.* **2013**, *46*, 792-801.

(16) Aznar, E.; Oroval, M.; Pascual, L.; Murguía, J. R.; Martínez-Máñez, R.; Sancenón, F. Gated Materials for On-Command Release of Guest Molecules. *Chem. Rev.* **2016**, *116*, 561-718.

(17) Song, N.; Yang, Y.-W. Molecular and Supramolecular Switches on Mesoporous Silica Nanoparticles. *Chem. Soc. Rev.* **2015**, *44*, 3474-3504.

(18) Lv, Y.; Cao, Y.; Li, P.; Liu, J.; Chen, H.; Liu, W.; Zhang, L. Ultrasound-Triggered Destruction of Folate-Functionalized Mesoporous Silica Nanoparticle-Loaded Microbubble for Targeted Tumor Therapy. *Adv. Healthcare Mater.* **2017**, *6*, 1700354.

(19) Martínez-Carmona, M.; Lozano, D.; Baeza, A.; Colilla, M.; Vallet-Regí, M. A Novel Visible Light Responsive Nanosystem for Cancer Treatment. *Nanoscale* **2017**, *9*, 15967-15973.

(20) Tarn, D.; Ferris, P.; Barnes, J. C.; Ambrogio, M. W.; Stoddart, J. F.; Zink, J. I. A Reversible Light-Operated Nanovalve on Mesoporous Silica Nanoparticles. *Nanoscale* **2014**, *6*, 3335-3343.

(21) Lu, C.-H.; Willner, I. Stimuli-Responsive DNA-Functionalized Nano-/Microcontainers for Switchable and Controlled Release. *Ang. Chem. Int. Ed.* **2015**, *54*, 12212-12235.

(22) Gisbert-Garzarán, M.; Lozano, D.; Vallet-Regí, M.; Manzano, M. Self-Immolative Polymers as Novel pH-Responsive Gate Keepers for Drug Delivery. *RSC Adv.* **2017**, *7*, 132-136.

(23) Llopis-Lorente, A.; Lozano-Torres, B.; Bernardos, A.; Martínez-Máñez, R.; Sancenón, F. Mesoporous Silica Materials for Controlled Delivery Based on Enzymes. *J. Mater. Chem. B* **2017**, *5*, 3069-3083.

(24) Sancenón, F.; Pascual, L.; Oroval, M.; Aznar, E.; Martínez-Máñez, R. Gated Silica Mesoporous Materials in Sensing Applications. *ChemistryOpen* **2015**, *4*, 418-437.

(25) Llopis-Lorente, A.; Díez, P.; de la Torre, C.; Sánchez, A.; Sancenón, F.; Aznar, E.; Marcos, M. D.; Martínez-Ruíz, P.; Martínez-Máñez, R.; Villalonga, R. Enzyme-Controlled Nanodevice for Acetylcholine-Triggered Cargo Delivery Based on Janus Au–Mesoporous Silica Nanoparticles. *Chem. Eur. J.* **2017**, *23*, 4276-4281.

(26) Ding, C.; Tong, L.; Fu, J. Quadruple Stimuli-Responsive Mechanized Silica Nanoparticles: A Promising Multifunctional Nanomaterial for Diverse Applications. *Chem. Eur. J.* **2017**, *23*, 15041-15045.

(27) Llopis-Lorente, A.; de Luis, B.; García-Férnández, A.; Díez, P.; Sánchez, A.; Marcos, M. D., Villalonga, R.; Martínez-Máñez, R., Sancenón, F. Au–Mesoporous Silica Nanoparticles Gated with Disulfide-Linked Oligo(Ethylene Glycol) Chains for Tunable Cargo Delivery Mediated by an Integrated Enzymatic Control Unit. *J. Mater. Chem. B* **2017**, *5*, 6734-6740.

(28) Manesh, K. M.; Halámek, J.; Pita, M.; Zhou, J.; Tam, T. K.; Santhosh, P.; Chuang, M.-C.; Windmiller, J. R.; Abidin, D.; Katz, E.; Wang, J. Enzyme Logic Gates for the Digital Analysis of Physiological Level Upon Injury. *Biosens. Bioelectron.* **2009**, *24*, 3569-3574.

(29) Zhou, J.; Halamek, J.; Bocharova, V.; Wang, J.; Katz. E. Bio-Logic Analysis of Injury Biomarker Patterns in Human Serum Samples. *Talanta* **2011**, *83*, 955-959.

(30) Chen, M.; Huang, C.; He, C.; Zhu, W.; Xu, Y.; Lu, Y. A Glucose-Responsive Controlled Release System Using Glucose Oxidase-Gated Mesoporous Silica Nanocontainers. *Chem. Commun.* **2012**, *48*, 9522–9524.

(31) Wu, S.; Huang, X.; Du, X. Glucose- and pH-Responsive Controlled Release of Cargo from Protein-Gated Carbohydrate-Functionalized Mesoporous Silica Nanocontainers. *Angew. Chem. Int. Ed.* **2013**, *52*, 5580-5584.

(32) Oroval, M.; Díez, P.; Aznar, A.; Coll, C.; Marcos, M. D.; Villalonga, R.; Martínez-Máñez, R. Self-Regulated Glucose-Sensitive Neoglycoenzyme-Capped Mesoporous Silica Nanoparticles for Insulin Delivery. *Chem. Eur. J.* **2017**, *23*, 1353-1360.

(33) Adekola, K.; Rosen, S. T.; Shanmugam, M. Glucose Transporters in Cancer Metabolism. *Curr. Opin. Oncol.* **2012**, *24*, 650-654.

(34) da Veiga Moreira, J.; Hamraz, M.; Abolhassani, M.; Bigan, E.; Pèrés, S.; Pauvelé, L.; Nogueira, M. L.; Steyaert, J.-M.; Schwartz, L. The Redox Status of Cancer Cells Supports Mechanisms behind the Warburg Effect. *Metabolites* **2016**, *6*, 33-44.

(35) Yousef, F. O.; Zughul, M. B.; Badwan, A. A. The Modes of Complexation of Benzimidazole with Aqueous β-Cyclodextrin Explored by Phase Solubility, Potentiometric Titration, ^{1}H-NMR and Molecular Modeling Studies. *J. Incl. Phenom. Macrocycl. Chem.* **2007**, *57*, 519-523.

(36) Jerez, G.; Kaufman, G.; Prystai, M.; Schenkeveld, S.; Donkor, K. K.; Determination of Thermodynamic pK_a Values of Benzimidazole and Benzimidazole Derivatives by Capillary Electrophoresis. *J. Sep. Sci.* **2009**, *32*, 1087-1095.

(37) Rodwell, V. W.; Bender, D. A.; Botham, K. M.; Kennelly, P. J.; Weil, P. A. Harper's Illustrated Biochemistry, 30th Edition, Mc Graw Hill, **2015**, pp. 477.

(38) Xu, J.; Huang, P.; Qin, Y.; Jiang, D.; Chen, H. Analysis of Intracellular Glucose at Single Cells using Electrochemiluminescence Imaging. *Anal Chem* **2016**, *88*, 4609-4612.

(39) Zhang, Q.; Piston, D.W.; Goodman, R.H. Regulation of Corepressor Function by Nuclear NADH. Science **2002**, *295*, 1895-1897.

(40) Williamson, D.H., Lund P., Krebs H.A. The Redox State of Free Nicotinamide-Adenine Dinucleotide in the Cytoplasm and Mitochondria of Rat Liver. *Biochem. J.* **1967**, *103,* 514-527.

(41) Yamada, K.; Hara, N.; Shibata, T.; Osago, H.; Tsuchiya, M. The Simultaneous Measurement of Nicotinamide Adenine Dinucleotide and Related Compounds by Liquid

Chromatography/Electrospray Ionization Tandem Mass Spectrometry. Anal. Biochem **2006**, *352*, 282-285.

(42) Yang, H.; Yang, T.; Baur, J. A.; Perez, E.; Matsui, T.; Carmona, J.J.; Lamming, D. W.; Souza-Pinto, N.C.; Bohr V.A.; Rosenzweig, A.; de Cabo, R.; Sauve, A.A.; Sinclair, D. A. Nutrient-Sensitive Mitochondrial NAD^+ Levels Dictate Cell Survival. *Cell* **2007**, *130* 1095-1107.

(43) Llopis-Lorente, A.; Díez, P; Sánchez, A.; Marcos, M. D.; Sancenón, F.; Martínez-Ruíz, P.; Villalonga, R.; Martínez-Máñez, R. Toward Chemical Communication Between Nanodevices. *Nano Today* **2018**, *18*, 8-11.

(44) Llopis-Lorente, A.; Díez, P; Sánchez, A.; Marcos, M. D.; Sancenón, F.; Martínez-Ruíz, P.; Villalonga, R.; Martínez-Máñez, R. Interactive Models of Communication at the Nanoscale Using Nanoparticles that Talk to One Another. *Nat. Commun.* **2017**, *8*, 15511.

(45) Bonabeau, E.; Theraulaz, G.; Dorigo, M. *Swarm Intelligence: From Natural to Artificial Systems*, Oxford University Press, **1999.**

Table of Contents